

Ground-state phases in spin-crossover chains

Carsten Timm^{1,*} and Ulrich Schollwöck²

¹*Institut für Theoretische Physik, Freie Universität Berlin, Arnimallee 14, D-14195 Berlin, Germany*

²*Institut für Theoretische Physik C, RWTH Aachen, D-52056 Aachen, Germany*

(Received 28 October 2004; revised manuscript received 22 February 2005; published 21 June 2005)

Spin-crossover molecules having a low-spin ground state and a low-lying excited high-spin state are promising components for molecular electronics. We theoretically examine one-dimensional spin-crossover chain molecules of the type of Fe^{2+} triazole complexes. The existence of the additional low-spin/high-spin degree of freedom leads to rich behavior already in the ground state. We obtain the complete ground-state phase diagram, taking into account an elastic nearest-neighbor interaction, a ferromagnetic or antiferromagnetic exchange interaction between the magnetic ions, and an external magnetic field. Ground-state energies are calculated with high numerical precision using the density-matrix renormalization group. Besides pure low-spin, high-spin, and alternating low-spin/high-spin phases we obtain a number of periodic ground states with longer periods, which we discuss in detail. For example, for antiferromagnetic coupling there exists a dimer phase with a magnetic unit cell containing two high-spin ions forming a spin singlet and a single low-spin ion, which is stabilized by the energy gain for singlet formation.

DOI: 10.1103/PhysRevB.71.224414

PACS number(s): 75.10.Jm, 75.50.Xx, 85.65.+h

I. INTRODUCTION

One of the most active fields of materials science to emerge in recent years is *molecular electronics*,^{1,2} which proposes to use individual molecules as electronic components. A related idea is to use a single quantum spin, say of an ion, to store information. Kahn and co-workers³⁻⁵ have emphasized that *spin-crossover compounds*⁶⁻¹⁰ (SCCs) are particularly promising for molecular memory devices. These compounds consist of complexes involving transition-metal ions and organic ligands.⁷⁻¹⁰ The magnetic ions can be either in a low-spin (LS) or high-spin (HS) state, i.e., for the spin operator \mathbf{S}_i at site i the eigenvalues of $\mathbf{S}_i \cdot \mathbf{S}_i$ are $S_{\text{LS}}(S_{\text{LS}}+1)$ and $S_{\text{HS}}(S_{\text{HS}}+1)$ in the LS and HS state, respectively. The energy difference between HS and LS states is due to the competition between the crystal field splitting, which prefers doubly occupied d orbitals and, hence, LS, and Hund's first rule, which favors the HS state.⁷⁻¹⁰ In SCCs the LS state is the ground state and the HS state is at a moderate (thermal) excitation energy. SCCs show a characteristic crossover from the LS ground state to dominantly HS behavior at higher temperatures⁶ due to the higher degeneracy of the HS state. This crossover is typically sharper than expected for noninteracting magnetic ions and is even replaced by a first-order transition in several compounds.⁷⁻¹⁰ Spin-crossover phenomena are also observed in organic radicals¹¹ and certain inorganic transition-metal compounds.¹²

Of the large number of known SCCs some naturally form one-dimensional chains, for example Fe^{2+} with 4-R-1,2,4-triazole ligands.^{4,13} Three ligands form bridges between two adjacent iron ions. Other SCCs consist of two-dimensional layers, for example $\text{TiSr}_2\text{CoO}_5$.^{12,14}

Besides possible applications,³⁻⁵ SCCs are also interesting from a statistical-physics point of view. Compared to conventional local-moment systems they introduce an additional Ising degree of freedom σ_i , which distinguishes between the LS ($\sigma_i = +1$) and HS ($\sigma_i = -1$) states. In the case of a *diamag-*

netic LS state ($S_{\text{LS}}=0$) the low spins are essentially switched off. These SCCs are thus related to site-diluted spin models,¹⁵⁻¹⁷ but in our case the presence or absence of a spin is a *dynamical* variable and not a type of quenched disorder. Also related are recent studies of magnetic models with mobile vacancies¹⁸ and of insulating phases of atoms with spin in optical lattices.¹⁹ We show below that there is also a close relation to finite antiferromagnetic spin chains.

Antiferromagnetic spin chains have attracted a lot of interest since Haldane's (in the meantime firmly established) conjecture of a fundamental difference between (isotropic) half-integer and integer quantum spin chains.²⁰ Among other things, the latter always show an excitation gap, while the former are critical. The valence-bond-solid model (AKLT model),²¹ in which each spin of length S is replaced by $2S$ fully symmetrized spin-1/2 objects that are then linked by singlet bonds between sites, was found to explain all main features of integer quantum spin chains. One peculiarity of the AKLT model is that at each end of *open* spin chains S of the spin-1/2 objects find no singlet partner and form a free spin $S/2$. For integer spins this leads in the AKLT model for *even* chain lengths to a $[2(S/2)+1]^2=(S+1)^2$ -fold degenerate ground state instead of the nondegenerate ground state found for periodic boundary conditions. This observation carries over to antiferromagnetic Heisenberg chains. There, one finds a group of $(S+1)^2$ low-lying states that become degenerate exponentially fast for long open chains. The lowest lying of these states has total spin 0; above this state there follows a spin-1 triplet, etc. The maximum total spin in this group of states is given by S and is concentrated at the edges. The lowest-lying excitation above them is a true bulk excitation and corresponds to the lowest-lying state with $M=S+1$. This phenomenon has been observed experimentally,²² and generates a wealth of low-lying excitations if there are segments of spin chains of various lengths like in SCCs with $S_{\text{LS}}=0$. For *odd* chain lengths, the situation is different as the lowest-lying states of the magnetization

sectors $M \leq S$ are strictly degenerate both in the AKLT and Heisenberg models. However, the ground state of the magnetization $S+1$ sector again contains the lowest-lying bulk excitation. This observation points to a special role of magnetization $M=S$, as will be seen throughout this paper.

In the present paper we focus on the ground-state properties of one-dimensional SCCs, for which we obtain essentially exact results. In particular, we treat the case of a diamagnetic LS state appropriate for Fe^{2+} ions. We mostly consider *antiferromagnetic* coupling between the spins, which is probably the more common situation.

II. THEORY

We start from the Hamiltonian²³

$$H_0 = -V \sum_{\langle ij \rangle} \sigma_i \sigma_j - B_0 \sum_i \sigma_i - h \sum_i S_i^z. \quad (1)$$

The sum over $\langle ij \rangle$ counts all nearest-neighbor bonds once and the eigenvalues of S_i^z are $m_i = -S_i, -S_i+1, \dots, S_i$, where $S_i = S_{\text{LS}} (S_{\text{HS}})$ for $\sigma_i = 1 (-1)$. V describes an interaction that for $V > 0$ ($V < 0$) favors homogeneous (alternating) arrangements of LS and HS. At least in a subset of known SCCs this interaction is of *elastic* origin²⁴ and can be of either sign.¹⁴ We approximate this interaction by a nearest-neighbor term. $2B_0 > 0$ describes the energy difference between HS and LS and h is the physical magnetic field with g factor and Bohr magneton absorbed. H_0 is diagonal in the basis of eigenstates of all $\mathbf{S}_i \cdot \mathbf{S}_i$ and S_i^z . In this basis²⁵

$$H_0 = -V \sum_{\langle ij \rangle} \sigma_i \sigma_j - B_0 \sum_i \sigma_i - h \sum_i m_i. \quad (2)$$

For $h=0$ we reobtain the Ising-type model introduced by Wajnflasz and Pick²⁶ for magnetic molecular compounds and by Doniach²⁷ for lipidic chains. Here, each site can be in two states characterized by σ_i like in the Ising model, but the states are degenerate with degeneracies $2S_{\text{LS}}+1$ and $2S_{\text{HS}}+1$.²⁸ The model can be rigorously mapped onto an Ising model in a temperature-dependent effective field B ^{23,27,29} and has been treated in the mean-field approximation and with Monte Carlo simulations.⁵ A related model with next-nearest-neighbor elastic interactions has recently been studied by Monte Carlo simulations and a number of stripe phases have been found.¹⁴ The one-dimensional model suitable for triazole compounds has not been treated before.

We are interested in a model with an additional exchange interaction $J \neq 0$ between the magnetic ions. The Hamiltonian (1) is generalized to

$$H = H_0 - J \sum_{\langle ij \rangle} \mathbf{S}_i \cdot \mathbf{S}_j, \quad (3)$$

where $J > 0$ ($J < 0$) corresponds to a ferromagnetic (antiferromagnetic) coupling between the spins. J has not been measured in SCCs, but it has been determined in similar metal-organic complexes. $|J|/k_B$ is typically of the order of 10–20 K and is antiferromagnetic,^{30–32} as expected for a kinetic superexchange interaction.³³ In compounds based on Prussian blue, larger exchange interactions have been ob-

served, leading to ferrimagnetic order at room temperature.³⁴

The full Hamiltonian H commutes with the operators $\mathbf{S}_i \cdot \mathbf{S}_i$. Thus the total spin *at each site* is a constant of motion. On the other hand, H does no longer commute with S_i^z . In the case of Fe^{2+} , which is the most common magnetic ion in SCCs, we have $S_{\text{HS}}=2$ and $S_{\text{LS}}=0$ and a significant simplification ensues, since any low spin partitions the chain into finite segments that do not interact *magnetically*. Thus there is a close relation to the physics of finite spin chains. In more than one dimension $S_{\text{LS}}=0$ leads to a less trivial percolation problem—for long-range order to be present it is necessary for the high spins to percolate.

In the following we restrict ourselves to $S_{\text{LS}}=0$. The Hamiltonian can be written as

$$H = -V \sum_i (\sigma_i \sigma_{i+1} - 1) - B_0 \sum_i (\sigma_i - 1) - J \sum_i \mathbf{S}_i \cdot \mathbf{S}_{i+1} - h \sum_i S_i^z, \quad (4)$$

where we have added a constant so that the energy of the pure LS state vanishes. The Ising operators σ_i all commute with the Hamiltonian H . Their eigenvalues are thus good quantum numbers and the Hilbert space is a direct product of subspaces for given $\{\dots, \sigma_i, \sigma_{i+1}, \dots\}$.²⁵

In each sector $\{\dots, \sigma_i, \sigma_{i+1}, \dots\}$ the system consists of chains of high spins separated by chains of low spins. The pure HS and LS states are obtained as the obvious limits. Since the LS chains do not contribute to the energy, the total energy in a sector can be written as a sum over the energies of HS chains of various lengths, including a contribution from their ends. These HS chains do not interact magnetically since $S_{\text{LS}}=0$.

We are interested in the ground state and thus consider the *lowest* energy in each sector. The lowest energy in a sector can be written as the sum over the ground-state energies of noninteracting finite HS chains. Since H commutes with the total spin of each HS chain separately, the z -components M of the total spins of the finite chains are good quantum numbers. Let us denote the lowest energy of a HS chain of length n with magnetic quantum number M by $e_n^0(M)$, where $|M| \leq nS_{\text{HS}}$. We write

$$e_n^0(M) = 4V + 2nB_0 - hM + \Delta e_n^0(M), \quad (5)$$

where the first term comes from the extra energy of the change from HS to LS at the ends. The final term is the lowest eigenenergy of the finite HS Heisenberg chain with open boundary conditions and the Hamiltonian $H_n = -J \sum_{i=1}^{n-1} \mathbf{S}_i \cdot \mathbf{S}_{i+1}$.

III. RESULTS AND DISCUSSION

A. Ferromagnetic coupling

For ferromagnetic coupling, $J > 0$, and magnetic field $h > 0$ both the exchange interaction and the Zeeman term favor ferromagnetic alignment. The lowest-energy state thus has the maximum magnetic quantum number $M = nS_{\text{HS}}$ for each chain. For $J \geq 0$ we have $\Delta e_n^0(nS_{\text{HS}}) = -(n-1)JS_{\text{HS}}^2$ and thus

$$e_n^0(nS_{\text{HS}}) = 4V + 2nB_0 - nhS_{\text{HS}} - (n-1)JS_{\text{HS}}^2. \quad (6)$$

Now let us consider a sector $\{\dots, \sigma_i, \sigma_{i+1}, \dots\}$ for which the state consists of *volume fractions* p_n of HS chains of length n . The HS chains have to be separated by at least one low spin. When counting this low spin with each HS chain, the volume fractions become $(n+1)/np_n$. They must satisfy the constraint

$$\sum_{n=1}^{\infty} \frac{n+1}{n} p_n \leq 1. \quad (7)$$

The energy per site is

$$\begin{aligned} \epsilon_0 &= \sum_n p_n \frac{e_n^0(nS_{\text{HS}})}{n} \\ &= \sum_n p_n \left(\frac{4V + JS_{\text{HS}}^2}{n} + 2B_0 - hS_{\text{HS}} - JS_{\text{HS}}^2 \right). \end{aligned} \quad (8)$$

We have to solve the linear optimization problem of minimizing ϵ_0 under the constraint (7). In the space of vectors (p_1, p_2, \dots) the region allowed by Eq. (7) is a hyperpyramid with apex at zero and the other corners at points with $p_m = m/(m+1)$ for one m and $p_n = 0$ for $n \neq m$. These are the points for which only chains of one single length are present and have the maximum volume fraction. This means that the finite HS chains are separated by *single* low spins. Since the allowed region is convex, the only possible solutions are its corners, except for special choices of parameters. Thus either $p_n = 0$ for all n (LS state) or $p_m = m/(m+1)$ for one m and all other $p_n = 0$. For the LS state we have $\epsilon_0 = 0$, whereas for the state with nonzero p_n ,

$$\epsilon_0 = \frac{4V - 2B_0 + 2JS_{\text{HS}}^2 + hS_{\text{HS}}}{n+1} + 2B_0 - hS_{\text{HS}} - JS_{\text{HS}}^2. \quad (9)$$

Examination shows that there are only three possible phases: (i) If $4V - 2B_0 + 2JS_{\text{HS}}^2 + hS_{\text{HS}} > 0$ and $2B_0 - hS_{\text{HS}} - JS_{\text{HS}}^2 > 0$ or $4V - 2B_0 + 2JS_{\text{HS}}^2 + hS_{\text{HS}} < 0$ and $2V + B_0 - hS_{\text{HS}}/2 > 0$ the ground state is the LS state. (ii) If $4V - 2B_0 + 2JS_{\text{HS}}^2 + hS_{\text{HS}} > 0$ and $2B_0 - hS_{\text{HS}} - JS_{\text{HS}}^2 < 0$ the ground state has $p_n > 0$ and all other $p_m = 0$, for $n \rightarrow \infty$, which corresponds to the HS state, and the energy is $\epsilon_0 = 2B_0 - hS_{\text{HS}} - JS_{\text{HS}}^2$. Note that the HS state appears for any values of V and h for sufficiently large exchange interaction J . This is reminiscent of the exchange-induced Van-Vleck ferromagnetism in rare-earth compounds.³⁵ (iii) If $4V - 2B_0 + 2JS_{\text{HS}}^2 + hS_{\text{HS}} < 0$ and $2V + B_0 - hS_{\text{HS}}/2 < 0$ the ground state has $p_1 = 1/2$ and all other $p_m = 0$. This corresponds to an *alternating* state of low and high spins. The energy is $\epsilon_0 = 2V + B_0 - hS_{\text{HS}}/2$. By using the LS/HS splitting B_0 as our unit of energy, we obtain the phase diagram in V/B_0 , h/B_0 , and J/B_0 shown as the $J \geq 0$ part of Fig. 8, below.

B. Antiferromagnetic coupling

In the case of antiferromagnetic coupling, $J < 0$, there is a competition between the exchange and Zeeman terms in Eq. (4). Thus in principle finite HS chains of length n can occur

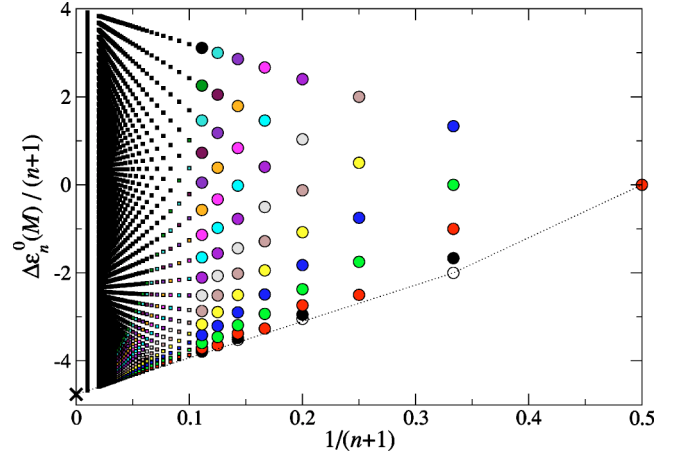


FIG. 1. (Color online) The lowest energies $\Delta e_n^0(M)/|J|$ of antiferromagnetic Heisenberg chains of length n for spin $S_{\text{HS}}=2$ in sectors with open boundary conditions for fixed total S^z quantum number M . The energies are normalized by a factor $1/(n+1)$ and shown as a function of $1/(n+1)$, where $n+1$ is the period of the LS/HS pattern. Circles: Results from exact Lanczos diagonalization. Squares: Results from DMRG. Equal colors correspond to equal M . For odd n the energies for $M=0, 1$, and 2 are degenerate, as noted in Sec. I. The cross at $1/(n+1)=0$ denotes the extrapolated energy density $-4.761248(1)$ of an infinite chain (see Ref. 36).

with any magnetic quantum number M . The energy $e_n^0(M)$ of such a chain is given by Eq. (5). We introduce volume fractions $p_{n,M}$ of HS chains of length n with magnetic quantum number M . They must satisfy the constraint

$$\sum_{n=1}^{\infty} \sum_{M=-nS_{\text{HS}}}^{nS_{\text{HS}}} \frac{n+1}{n} p_{n,M} \leq 1. \quad (10)$$

The energy per site is

$$\epsilon_0 = \sum_{n,M} p_{n,M} \left(\frac{4V - hM + \Delta e_n^0(M)}{n} + 2B_0 \right). \quad (11)$$

The ground state for certain parameter values is determined by the minimum of ϵ_0 under the constraint (10). This is again a linear optimization problem. Except for accidental degeneracies, the minima occur at the corners of the allowed parameter region. Thus either $p_{n,M} = 0$ for all (n, M) (LS state) or $p_{n,M} = n/(n+1)$ for one (n, M) and $p_{n,M} = 0$ for all others. In the latter case the energy per site is

$$\epsilon_0 = \frac{4V - 2B_0 - hM + \Delta e_n^0(M)}{n+1} + 2B_0. \quad (12)$$

$\Delta e_n^0(M)/|J|$ is the lowest energy of the finite antiferromagnetic Heisenberg chain with open boundary conditions and the Hamiltonian $H'_n = \sum_{i=1}^{n-1} \mathbf{S}_i \cdot \mathbf{S}_{i+1}$ in the sector with total S^z quantum number M . It is not possible to find these energies in analytical form. For sufficiently small n , the Hamiltonian H'_n can be diagonalized numerically. We have calculated the energies up to $n=8$ for all M using the Lanczos algorithm. The results for $\Delta e_n^0(M)/|J|/(n+1)$ are shown in Fig. 1 as

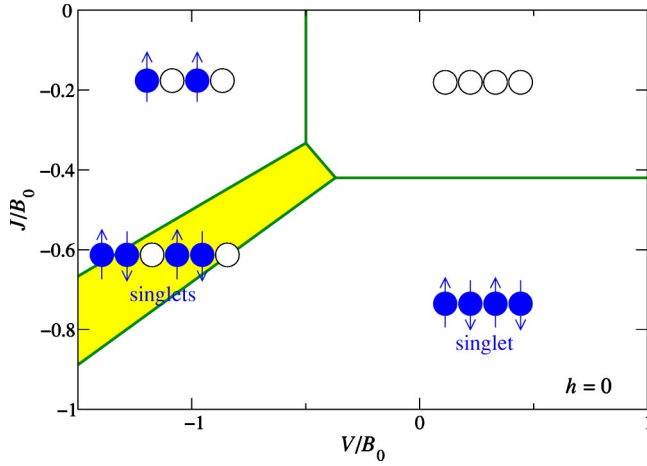


FIG. 2. (Color online) Ground-state phase diagram of the one-dimensional (1D) spin-crossover model with $S_{\text{LS}}=0$ and $S_{\text{HS}}=2$ for vanishing magnetic field, $h=0$, and antiferromagnetic exchange interaction, $J<0$. The dimer ($n=2$) phase case is highlighted. The heavy solid lines denote discontinuous transitions. The various spin structures are indicated by cartoons (solid symbols: HS state, open symbols: LS state); these should not be overinterpreted—there is no magnetic long-range order.

colored circles, where identical colors denote the same values of M .

The energies for longer chains can be calculated with excellent precision with a finite-chain density-matrix renormalization group (DMRG) algorithm;^{37,38} for a detailed explanation of the algorithm and its applications see Refs. 39 and 40. To obtain typically seven-digit precision for the ground state energy per site, we have kept up to $M=300$ states in the reduced DMRG Hilbert spaces and carried out three finite-system sweeps which was enough to ensure convergence. Note that DMRG prefers open to periodic boundary conditions. In standard DMRG applications to integer-spin chains, end spins of length $S/2$ (a spin 1 at each end for our case) are attached to eliminate the peculiar boundary degrees of freedom and access bulk physics directly.^{37,41} In the present calculation, these boundary degrees of freedom are physical

and, hence, no end spins are attached. The energies for lengths $n=9$ through $n=49$ as well as $n=99$ are shown in Fig. 1 by squares.⁴²

We first consider the case of *vanishing magnetic field*, $h=0$. Figure 1 shows that the state with $M=0$ has the lowest energy for any n . Then $\epsilon_0=[4V-2B_0+\Delta e_n^0(0)]/(n+1)+2B_0$ is a sum of $\Delta e_n^0(0)/(n+1)$ and a *linear* function in $1/(n+1)$. The minimum of ϵ_0 can only occur for $n=1$, $n=2$, or $n\rightarrow\infty$, since all other points lie above the dotted straight lines connecting the corresponding points in Fig. 1 (not obvious on this scale). The relevant energies per site are thus determined by $\Delta e_1^0/2=0$, $\Delta e_2^0/3=2J$, and $\lim_{n\rightarrow\infty} \Delta e_n^0/(n+1)=4.761248J$ and have to be compared to the LS energy $\epsilon_0=0$. The resulting phase diagram is shown in Fig. 2. Note the appearance of a *dimer* ($n=2$) phase. In this phase the energy increase due to the HS-HS pairs ($V<0$ favors HS-LS neighbors) is overcompensated by the large negative singlet formation energy of Heisenberg spin pairs.

For *general magnetic field* h we have to take all possible magnetic quantum numbers M of the chains into account. This is obviously impossible for the pure HS phase. Instead, we have performed DMRG calculations for chain length $n=99$ for all possible magnetizations $M=0, \dots, 198$ and use them as a caricature of the HS state. The resulting errors are discussed below.

For each set of parameters $(V/B_0, J/B_0, h/B_0)$ we calculate the minimum energy densities for all states with $n\leq 49$ as well as $n=99$ from Eq. (12). The energy density of the LS state is zero. Then the ground state is obtained by finding the minimum energy. Figure 3 shows a series of phase diagrams for fixed exchange interaction J . Note that the lower edges of each diagram, i.e., $h=0$, are consistent with Fig. 2. We observe that the dimer ($n=2$) phase present at $h=0$ is suppressed by the field, as is expected since this phase is stabilized by the singlet formation energy.

For $J\lesssim -0.6$ the phase diagrams remain qualitatively the same. The features are shifted to lower V and expanded linearly in both the V and h directions. Letting V, J , and h go to infinity while keeping their ratios fixed corresponds to the limit $B_0\rightarrow 0$, i.e., vanishing energy difference between LS and HS states. In this limit we choose $|J|$ as our unit of

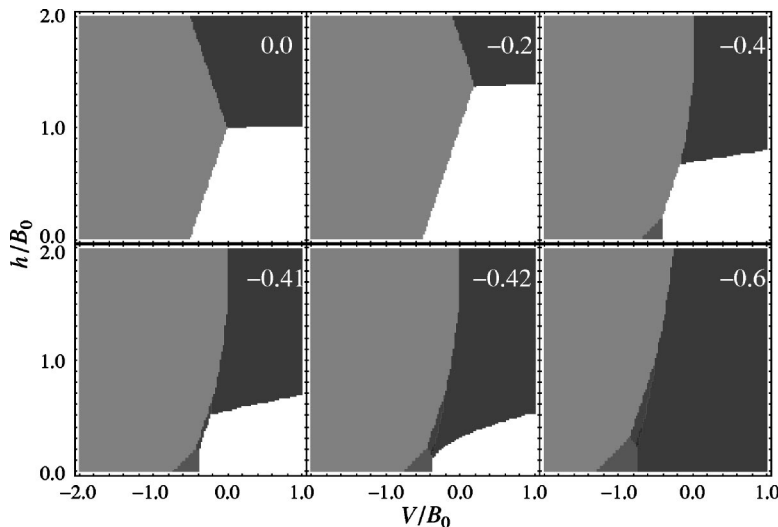


FIG. 3. Zero-temperature phase diagrams for the same model as in Fig. 2, but in a magnetic field, for antiferromagnetic exchange interactions $J/B_0=0.0, -0.2, -0.4, -0.41, -0.42, -0.6$. The white area corresponds to the LS phase, the black to the HS phase, approximated by a phase with $n=99$, and the gray areas correspond to $n=1, 2, 3, 5$ (from light to dark). All transition are discontinuous, the purely magnetic continuous transition discussed below is not shown.

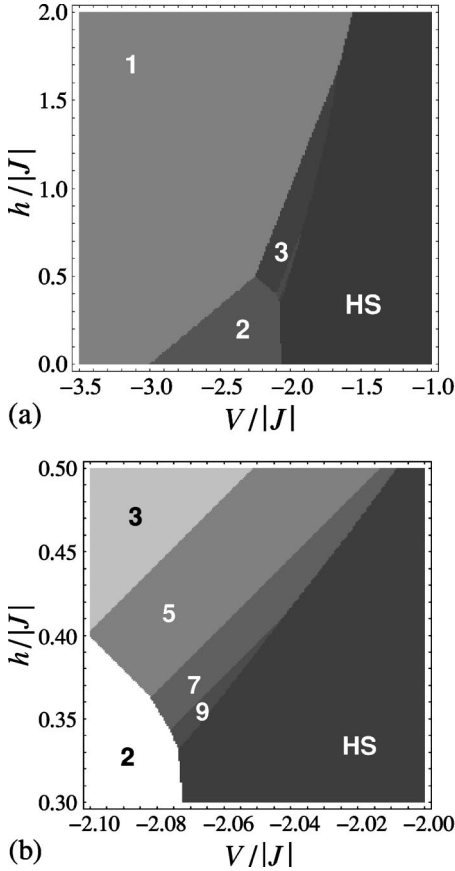


FIG. 4. (a) Zero-temperature phase diagrams as in Fig. 3 in the limit $B_0 \rightarrow 0$ (or $V, J, h \rightarrow \infty$ with their ratios fixed). The gray scale is the same as in Fig. 3. (b) Enlargement of the left figure on a *different gray scale*. The values of n in the various ground states are indicated.

energy, leaving two dimensionless parameters $V/|J|$ and $h/|J|$. The resulting phase diagram is shown in Fig. 4.

Interesting behavior is seen in the triangular region surrounded by phases with $n=1$, $n=2$, and the HS phase, as shown in Fig. 4(b). Here, phases with HS chain lengths $n=3, 5, 7$, and 9 are found. We do not observe any further phases. To understand why only *odd* n appear, we refer to the energy densities in Fig. 1: The energy of the singlet ($M=0$) state is *lower* for even n than expected from a linear fit, at least for the small n relevant here, while for odd n it is higher. Thus at zero magnetic field, even- n states are preferred. On the other hand, the energy of states with $M \geq 2$ is *higher* for even n than a linear fit, while for odd n it is lower. Thus in a sufficiently large magnetic field odd- n states are preferred. The fact that the series of odd n is cutoff at $n=9$ is a result of the detailed numerical values of energies in Fig. 1—for larger n , the HS state happens to have the lower energy. While we expect the appearance of only odd HS chain lengths to be a robust feature of spin-crossover chains with strong antiferromagnetic interaction, the restriction to $n \leq 9$ should thus be model dependent. For example, inclusion of a next-nearest-neighbor elastic interaction or a different integer value of S_{HS} may change this result.

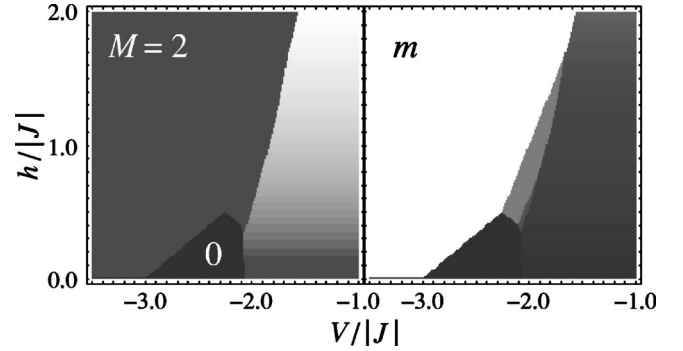


FIG. 5. Left: Density plot of the magnetic quantum number M of the finite chains in the same parameter region as in Fig. 4(a). Black corresponds to $M=0$, white to maximum M . The phases with odd n all have $M=2$. Right: Magnetization $m=M/(n+1)$ derived from the data in the left plot. Black (white) corresponds to $m=0$ ($m=1$). The magnetization of the fully polarized HS state, which does not appear in the plot, would be $m=S_{\text{HS}}=2$.

C. Magnetic properties

We now discuss the magnetic properties in more detail. In the ferromagnetic case all high spins are fully aligned with a nonzero magnetic field h . For the antiferromagnetic case Fig. 5 shows the magnetic quantum number M of the finite HS chains and the magnetization m in the ground states in the limit of large V, J, h . The magnetization is defined as the magnetic quantum number M divided by the period, $m=M/(n+1)$. Interestingly, the phases with odd n all have $M=S_{\text{HS}}=2$, including the $n=7$ and $n=9$ phases not resolved in Fig. 5. This of course corresponds to different *magnetizations* m . To understand the special significance of the value $M=S_{\text{HS}}$, we plot in Fig. 6 the local expectation values of the spins, $\langle S_i^z \rangle$, for each site of a HS chain of length $n=9$, obtained with DMRG. The plot shows that for $0 < M \leq S_{\text{HS}}$ the *odd* chain can accommodate the finite spin by forming a Néel-type state. For higher M this is no longer possible and spins pointing in the “wrong” direction are reduced (a bulk magnon is excited). Due to the cost in exchange energy such states are always higher in energy than competing phases. Compare also the discussion in Sec. I.

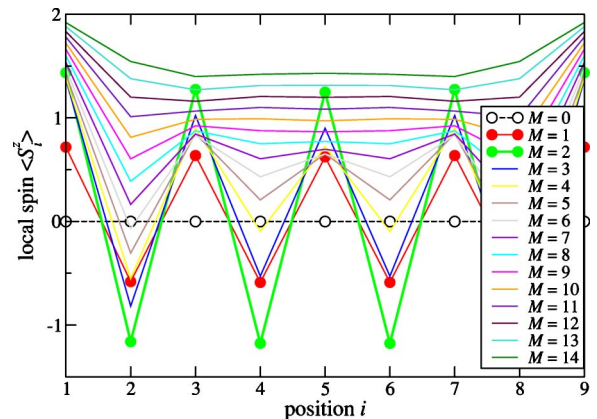


FIG. 6. (Color online) Local expectation values $\langle S_i^z \rangle$ from DMRG for each site of a HS chain of length $n=9$ for various total magnetic quantum numbers of the chain, M .

The dimer ($n=2$) phase always consists of singlets, $M=0$. This shows that it is energetically favorable to replace the dimer state by a state with odd n or the HS state, instead of having $M>0$ for the dimers.

Finally, we turn to the pure HS phase. At $T=0$ the system is equivalent to an infinite antiferromagnetic $S=S_{\text{HS}}$ chain. We thus expect the magnetization to rise continuously with increasing magnetic field h and to reach its maximum value $m=S_{\text{HS}}$, i.e., full spin alignment, at a *continuous* phase transition. Since we approximate the HS phase by the $n=99$ phase, the continuous increase is replaced by small steps. The position of this transition is determined by equating the energies per site for $M=nS_{\text{HS}}$ and $M=nS_{\text{HS}}-1$. From Eq. (12) we thus obtain the critical field $h_c=\Delta e_n^0(2n)-\Delta e_n^0(2n-1)$, which is proportional to J and independent of B_0 and V . For $n=99$ exact diagonalization yields $h_c\approx-7.9980J$, compared to the exact result for an infinite chain, $h_c=-4JS_{\text{HS}}=-8J$. To find the critical behavior close to this transition we define the deviation of the magnetization from its maximum by $\Delta m\equiv S_{\text{HS}}-m$. Plotting Δm^2 vs h (not shown) we find that Δm^2 is linear in h_c-h so that the critical exponent of Δm with respect to the field h is mean-field-like, $\beta=1/2$.

The previous discussion shows that by restricting the DMRG calculations to $n<100$ we make an error for the transition to full spin alignment of the order of 0.03%. As another way to estimate the errors, we have determined the triple point between LS, HS, and dimer phases in zero field and compared the result to the “exact” triple point shown in Fig. 2. The error is of the order of 0.2% for V and 0.1% for J .

We also obtain spin correlations from the DMRG. Figure 7 shows spin-spin correlation functions for $n=99$ for two

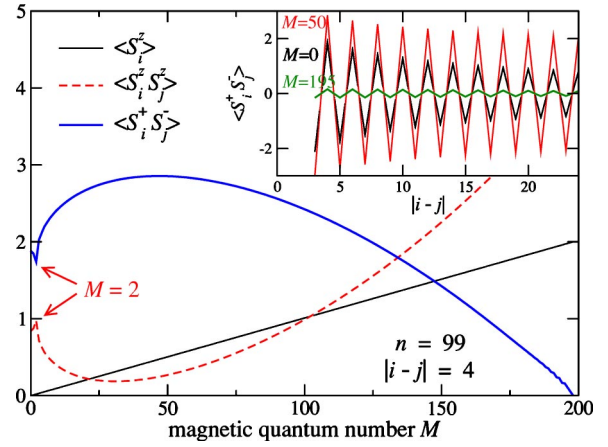


FIG. 7. (Color online) Expectation value of the z component of the spins, $\langle S^z \rangle$, and spin-spin correlation functions at the separation of $|i-j|=4$ as functions of the total magnetic quantum number M for chain length $n=99$. Inset: Correlation function $\langle S_i^+ S_j^- \rangle$ as a function of separation for three values of the total magnetic quantum number M .

spins close to the center of the chain, where the infinite chain should be well approximated. We first notice the anomaly at $M=2$. This is of the same origin as the stabilization of $M=2$ for small odd chain lengths, discussed above. It is thus a finite-size effect not present for the true HS phase. Apart from this anomaly, the *transverse* correlations $\langle S_i^+ S_j^- \rangle$ first grow with magnetic field h or magnetization. This is the one-dimensional analog of the spin-flop state in ordered antiferromagnets, where the staggered magnetization is oriented perpendicularly to the applied field. For large fields, the correlations decrease again since the spins are more and

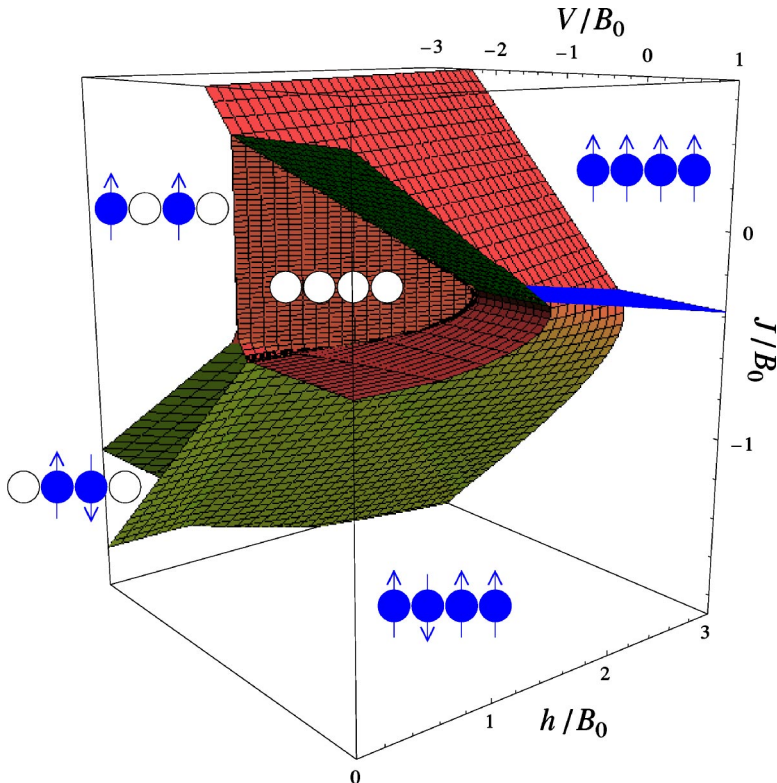


FIG. 8. (Color online) Zero-temperature phase diagram of the spin-crossover chain with $S_{\text{LS}}=0$ and $S_{\text{HS}}=2$. Positive (negative) J corresponds to ferromagnetic (antiferromagnetic) exchange interaction. V denotes the elastic interaction, h the applied magnetic field in units of energy, and $2B_0$ is the energy difference between HS and LS states in the absence of interactions. The solid surfaces denote phase transitions between different phases, which are indicated. The phases with HS chain lengths $n=3, 5, \dots$ are hidden in this view. All transitions are discontinuous, except for the continuous transition to full spin alignment in the HS phase, shown as the monochrome (blue) surface.

more forced into the field direction. In the fully polarized state for $h \geq h_c$ the transverse fluctuations vanish.

IV. SUMMARY AND CONCLUSIONS

To conclude, we have studied a model for spin-crossover compounds forming one-dimensional chains. We consider spin quantum numbers appropriate for Fe^{2+} ions, which have a spin-0 LS and a spin-2 HS state. The model includes elastic and exchange interactions and an applied magnetic field. The most important effect left out here is probably the dipole-dipole interaction, which is of long range for an isolated chain, but becomes screened if the chain is deposited on a conducting substrate. We obtain the ground-state phase diagram analytically for ferromagnetic or zero exchange interaction and using the DMRG for antiferromagnetic exchange. As a summary, Fig. 8 shows the full phase diagram. The continuous transition to full spin alignment is indicated by the solid blue surface. All other surfaces are discontinuous transitions between states with different chain length n . Horizontal cuts correspond to the plots in Fig. 3, the vertical cut at $h=0$ to Fig. 2. Besides a diamagnetic LS phase and a HS phase equivalent to the usual Heisenberg chain we find a number of more complex phases. For sufficiently negative elastic interaction V we find an alternating phase of low and high spins. In quasi-two-dimensional SCCs the corresponding checkerboard state has been observed experimentally.¹²

For antiferromagnetic coupling we find a robust dimer ($n=2$) phase, which consists of spin singlets formed by two

high spins separated by single low spins. Since this phase appears at zero and low magnetic fields, it should be accessible experimentally. As the magnetic field is increased, the dimers remain in the singlet state until states with an odd number of HS ions or the pure HS state become lower in energy, whereupon the dimer phase is destroyed in a discontinuous transition. At higher magnetic fields we find a number of phases consisting of finite chains of length $n = 3, 5, 7, 9$ of HS ions with total S^z quantum number $M=2$ separated by single LS ions. We suggest that the succession of odd chain lengths is a general feature of spin-crossover chains.

We thus find that a model that contains the most important ingredients of one-dimensional spin-crossover systems shows a rich ground-state phase diagram. The model is related to various systems studied in recent years, such as site-diluted spin models and finite antiferromagnetic Heisenberg chains. Questions for the future concern the behavior at non-zero temperature and of higher-dimensional models, in which *percolation* plays an important role. New physics comes into play since the dilution by LS ions is not quenched disorder but a dynamical degree of freedom.

ACKNOWLEDGMENTS

We would like to thank P. Gütlich, P. J. Jensen, and F. von Oppen for valuable discussions. C.T. thanks the Deutsche Forschungsgemeinschaft for support through Sonderforschungsbereich 290.

*Electronic address: timm@physik.fu-berlin.de

- ¹C. Joachim, J. K. Glimzewski, and A. Aviram, *Nature (London)* **408**, 541 (2000).
- ²A. Nitzan and M. A. Ratner, *Science* **300**, 1384 (2003).
- ³J. Zarembowitch and O. Kahn, *New J. Chem.* **15**, 181 (1991); O. Kahn, J. Krber, and C. Jay, *Adv. Mater. (Weinheim, Ger.)* **4**, 718 (1992).
- ⁴O. Kahn and C. Jay Martinez, *Science* **279**, 44 (1998).
- ⁵H. Bolvin and O. Kahn, *Chem. Phys.* **192**, 295 (1995); *Chem. Phys. Lett.* **243**, 355 (1995).
- ⁶L. Cambi and L. Szegö, *Ber. Dtsch. Chem. Ges. B* **64**, 259 (1931); **66**, 656 (1933).
- ⁷P. Gütlich, *Struct. Bonding (Berlin)* **44**, 83 (1981).
- ⁸E. König, *Struct. Bonding (Berlin)* **76**, 51 (1991).
- ⁹P. Gütlich, Y. Garcia, and H. A. Goodwin, *Chem. Soc. Rev.* **29**, 419 (2000).
- ¹⁰S. J. Blundell and F. L. Pratt, *J. Phys.: Condens. Matter* **16**, R771 (2004).
- ¹¹W. Fujita and K. Awaga, *Science* **286**, 261 (1999); M. E. Itkis, X. Chi, A. W. Cordes, and R. C. Haddon, *Science* **296**, 1443 (2002).
- ¹²M. Coutanceau, P. Dordor, J.-P. Doumerc, J.-C. Grenier, P. Maestro, M. Pouchard, D. Sedmidubsky, and T. Seguelong, *Solid State Commun.* **96**, 569 (1995); J.-P. Doumerc, J.-C. Grenier, P. Hagenmuller, M. Pouchard, and A. Villesuzanne, *J. Solid State Chem.* **147**, 211 (1999); J.-P. Doumerc, M. Coutanceau, A. De-

- mourgues, E. Elkaim, J.-C. Grenier, and M. Pouchard, *J. Mater. Chem.* **11**, 78 (2001).
- ¹³T. Yokoyama, Y. Murakami, M. Kiguchi, T. Komatsu, and N. Kojima, *Phys. Rev. B* **58**, 14238 (1998).
- ¹⁴D. L. Khomskii and U. Löw, *Phys. Rev. B* **69**, 184401 (2004).
- ¹⁵O. P. Vajk, P. K. Mang, M. Greven, P. M. Gehring, and J. W. Lynn, *Science* **295**, 1691 (2002).
- ¹⁶K. Kato, S. Todo, K. Harada, N. Kawashima, S. Miyashita, and H. Takayama, *Phys. Rev. Lett.* **84**, 4204 (2000); A. W. Sandvik, *Phys. Rev. Lett.* **86**, 3209 (2001); A. W. Sandvik, *Phys. Rev. B* **66**, 024418 (2002).
- ¹⁷R. Yu, T. Roscilde, and S. Haas, cond-mat/0410041 (unpublished).
- ¹⁸W. Selke, V. L. Pokrovsky, B. Büchner, and T. Kroll, *Eur. Phys. J. B* **30**, 83 (2002); R. Leidl and W. Selke, *Phys. Rev. B* **70**, 174425 (2004); M. Holtschneider, R. Leidl, and W. Selke, *J. Magn. Magn. Mater.* **290-291**, 326 (2005).
- ¹⁹A. Imambekov, M. Lukin, and E. Demler, *Phys. Rev. A* **68**, 063602 (2003); *Phys. Rev. Lett.* **93**, 120405 (2004).
- ²⁰F. D. M. Haldane, *Phys. Rev. Lett.* **50**, 1153 (1983).
- ²¹I. Affleck, T. Kennedy, E. H. Lieb, and H. Tasaki, *Phys. Rev. Lett.* **59**, 799 (1987).
- ²²M. Hagiwara, K. Katsumata, I. Affleck, B. I. Halperin, and J. P. Renard, *Phys. Rev. Lett.* **65**, 3181 (1990).
- ²³Y. Garcia, O. Kahn, J.-P. Ader, A. Buzdin, Y. Meurdesoif, and M. Guillot, *Phys. Lett. A* **271**, 145 (2000).

- ²⁴N. Willenbacher and H. Spiering, J. Phys. C **21**, 1423 (1988); J. Phys.: Condens. Matter **1**, 10089 (1989).
- ²⁵Here, σ_i is a quantum number, not an operator, but it is permissible to use the same symbol since the operator σ_i commutes with any other operator.
- ²⁶J. Wajnfłasz, Phys. Status Solidi **40**, 537 (1970); J. Wajnfłasz and R. Pick, J. Phys. (Paris), Colloq. **32**, C1-91 (1971).
- ²⁷S. Doniach, J. Chem. Phys. **68**, 4912 (1978).
- ²⁸The entropy change associated with the LS to HS transition is larger than predicted from these degeneracies due to the change in the vibrational properties between LS and HS states and can be taken into account by effective degeneracy factors (see Refs. 5 and 23).
- ²⁹M. Nielsen, L. Miao, J. H. Ipsen, O. G. Mouritsen, and M. J. Zuckermann, Phys. Rev. E **54**, 6889 (1996).
- ³⁰O. Waldmann, J. Hassmann, P. Müller, G. S. Hanan, D. Volkmer, U. S. Schubert, and J.-M. Lehn, Phys. Rev. Lett. **78**, 3390 (1997).
- ³¹C. Boskovic, A. Sieber, G. Chaboussant, H. U. Güdel, J. Enslin, W. Wernsdorfer, A. Neels, G. Labat, H. Stoeckli-Evans, and S. Janssen, Inorg. Chem. **43**, 5053 (2004).
- ³²T. Lancaster, S. J. Blundell, F. L. Pratt, M. L. Brooks, J. L. Manson, E. K. Brechin, C. Cadiou, D. Low, E. J. L. McInnes, and R. E. P. Winpenny, J. Phys.: Condens. Matter **16**, S4563 (2004).
- ³³P. W. Anderson, Phys. Rev. **79**, 350 (1950).
- ³⁴S. Ferlay, T. Mallah, R. Ouahès, P. Veillet, and M. Verdager, Nature (London) **378**, 701 (1995).
- ³⁵P. Fulde and I. Peschel, Adv. Phys. **21**, 1 (1972).
- ³⁶U. Schollwöck, O. Golinelli, and T. Jolicœur, Phys. Rev. B **54**, 4038 (1996).
- ³⁷S. R. White, Phys. Rev. Lett. **69**, 2863 (1992).
- ³⁸S. R. White, Phys. Rev. B **48**, 10345 (1993).
- ³⁹*Density Matrix Renormalization*, edited by I. Peschel, X. Wang, K. Hallberg, and M. Kaulke (Springer, New York, 1999).
- ⁴⁰U. Schollwöck, Rev. Mod. Phys. **77**, 259 (2005).
- ⁴¹U. Schollwöck and T. Jolicœur, Europhys. Lett. **30**, 493 (1995).
- ⁴²For $M=nS_{\text{HS}}-2$ and $M=nS_{\text{HS}}-1$ the results have been obtained by exact numerical diagonalization. For $M=nS_{\text{HS}}$ the exact analytical value $\Delta e_n^0(nS_{\text{HS}})/|J|=(n-1)S_{\text{HS}}^2$ has been used.